JTTEE5 12:560-571

Local and Global Fracture Toughness of a Flame Sprayed Molybdenum Coating

H.P. Brantner, R. Pippan, and W. Prantl

(Submitted 20 December 2001; in revised form 3 April 2002)

This study deals with the failure of a flame sprayed molybdenum coating and its fracture mechanical characterization. The microstructure of the coating was examined by scanning electron microscopy. Local hardness and Young's modulus values were measured by nanoindentation methods. X-ray measurements were used to estimate the grain size within the molybdenum splats. Special fracture mechanical tests were made to study the fracture mechanical behavior of cracks parallel and perpendicular to the coating-substrate interface. Indentation fracture toughness tests were made to examine the local fracture behavior of the material. Using these local toughness values and taking into account the microstructure, crack path, and mismatch effects it was possible to explain the global fracture toughness values.

Keywords flame spray, fracture toughness, microstructure, mismatch, molybdenum

1. Introduction

Molybdenum coatings are widely used in the automotive, shipping, aeronautical, and energy generating industry. Due to the tribological characteristics of molybdenum and its alloys, these coatings mostly are used to improve the wear resistance of components.[1-3] Especially in the automotive industry thermal sprayed molybdenum finds extensive applications on sliding contact surfaces such as piston rings, synchronizer rings etc. Thermal sprayed coatings fail as a result of the propagation and link-up of microcracks.[4] In this investigation the fracture mechanical behavior of thermal sprayed molybdenum was examined. Both the local and the global fracture properties are characterized to explain that behavior.

The material used in this study is a kind of composite material consisting of the coating and the substrate material. The behavior of cracks in composite materials is different from that in a homogeneous material.[5] The local conditions in front of a crack play a decisive role for the behavior of the crack. In a composite of materials with different mechanical properties three types of mismatch are very important for the behavior of the crack: elastic, plastic and thermal mismatch. They can increase or decrease the effective stress intensity at a crack leading to "shielding" or "antishielding," respectively.

2. Material

A case-hardened steel 16MnCr5 was coated with molybdenum by flame spraying. The impinging molybdenum droplets have cooling rates greater than 10^6 K/s[1] and form a relatively regular pancake structure. The "Mexican hat" shape of these "pancakes" (splats) was determined by stereophotogrammetry,[6,7] revealing a typical diameter of about 150 μm and a height of about 10 μm (Fig. 1). They form a layered structure as can be seen in the cross-sectional view of Fig. 2. Furthermore, Fig. 1 and 2 indicate that the splats contain a network of cracks, which are induced by the thermal shock occurring during the coating process. The thickness of the examined coatings ranges between 150 and 350 μm.

The fracture surface of a molybdenum splat as well as the surface of a splat at large magnification shows a very fine structure (Fig. 3). X-ray analysis reveals a mean grain size of 150-200 nm, which is in good agreement with the size of the substructure in Fig. 3. The fracture surface exhibits the anisitropic structure of the grains. This anisotropy can also be seen in the determined hardness values. On surfaces perpendicular to the interface we found about 300 HV and parallel to the interface about 760 HV. These values were determined at an indentation load of 50 N.

Taking into account that the yield stress of metallic materials is about three times its hardness, these hardness values correspond to a yield stress σ_y of about 900 and 2300 MPa. Using the Hall-Petch relation

$$\sigma_y = \sigma_0 + k_Y \cdot d^{-1/2} \quad \text{(Eq 1)}$$

where $\sigma_0 = 103$ MPa, $k_Y = 1.2$ MPa$\sqrt{m}$[8] and considering a grain size of 200 nm, gives a yield stress of 2700 MPa which is comparable to the yield stress obtained from hardness tests on the surface parallel to the interface.

The Young's modulus for homogeneous molybdenum is 325 GPa and the Poisson ratio is 0.3. If there are defects in the material (cracks or pores) the Young's modulus and the Poisson ratio may differ.[9-11] In nanoindentation tests with a maximum load of 9000 μN we measured a mean value of 290 GPa for the Young's modulus. With microhardness measurements (maximum load 500 mN) a value of 194 GPa was determined. For higher indentation loads the interaction volume becomes larger and the Young's modulus becomes smaller. Bending tests reveal

H.P. Brantner and **R. Pippan,** Erich-Schmid-Institut für Materialwissenschaften der Österreichischen Akademie der Wissenschaften, Jahnstrasse 12, A-8700 Leoben, Austria; and **W. Prantl,** Institut für Metallphysik der Montanuniversität Leoben, Jahnstrasse 12, A-8700 Leoben, Austria. Contact e-mail: akademie@unileoben.ac.at.

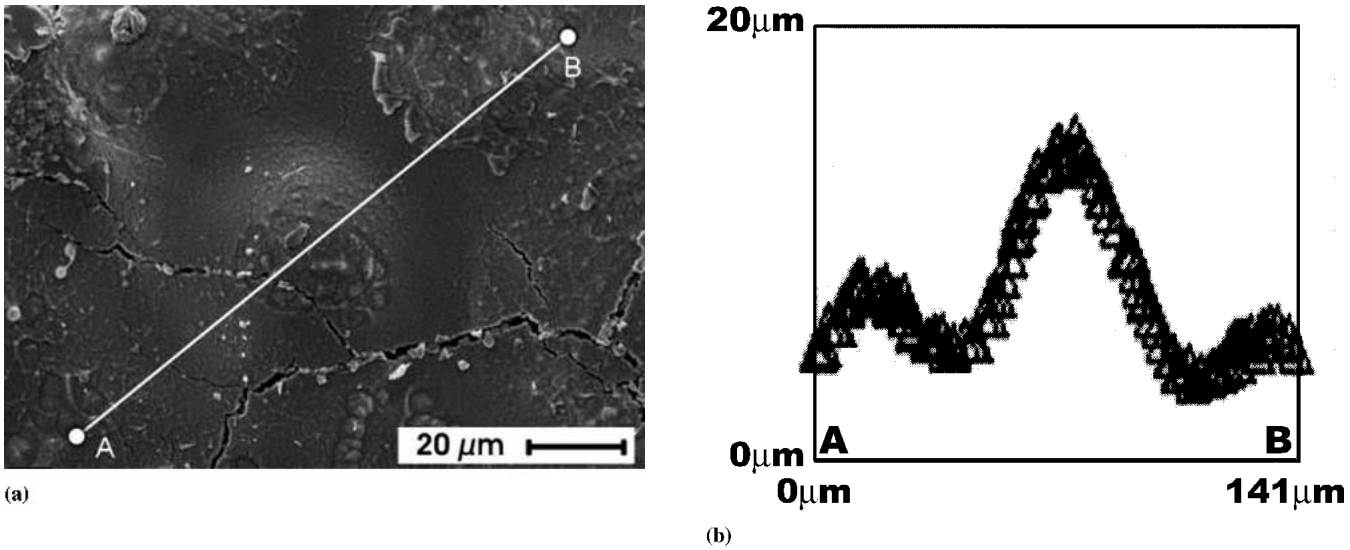

Fig. 1 Micrograph of the coating surface showing the shape of a "Mexican hat": **(a)** scanning electron image of the molybdenum surface, **(b)** height profile along the line A-B

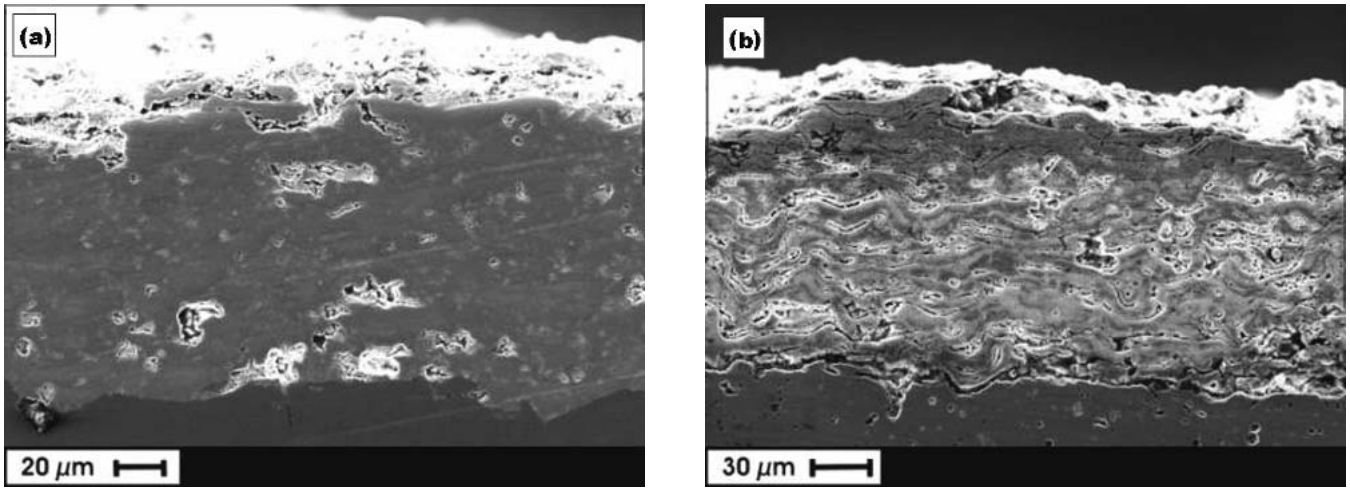

Fig. 2 Micrograph of the flame sprayed molybdenum coating: **(a)** cross section in the un-etched state, **(b)** cross section in the etched state

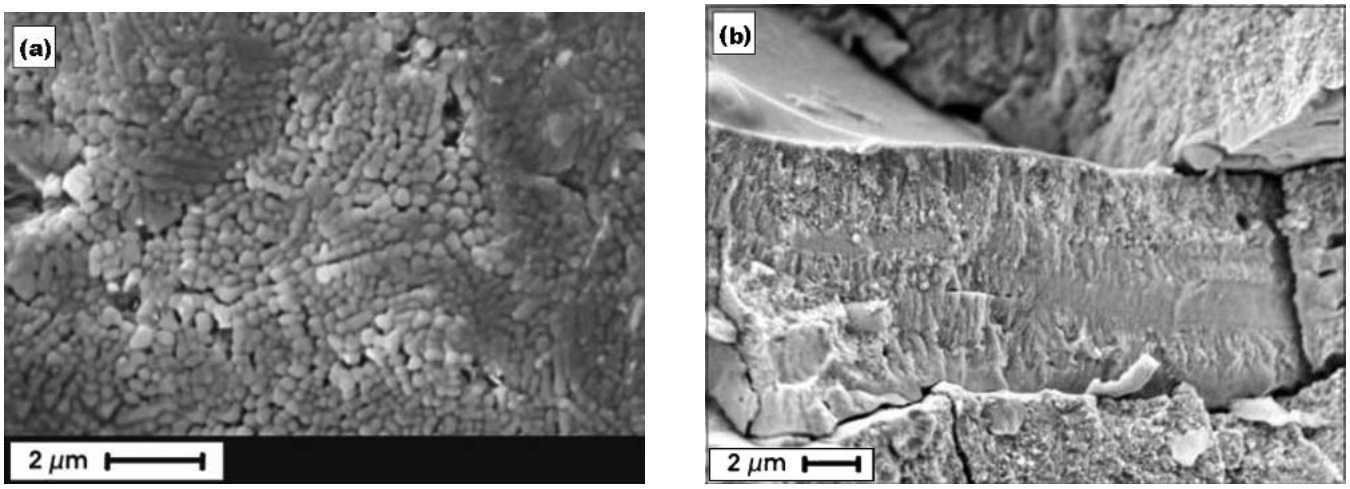

Fig. 3 Scanning electron micrographs (SEM) of molybdenum splats: **(a)** surface of a molybdenum splat; the microstructure of the splat shows a typical structure size of approximately 200 nm; **(b)** fracture surface of molybdenum splat showing the layer-like structure

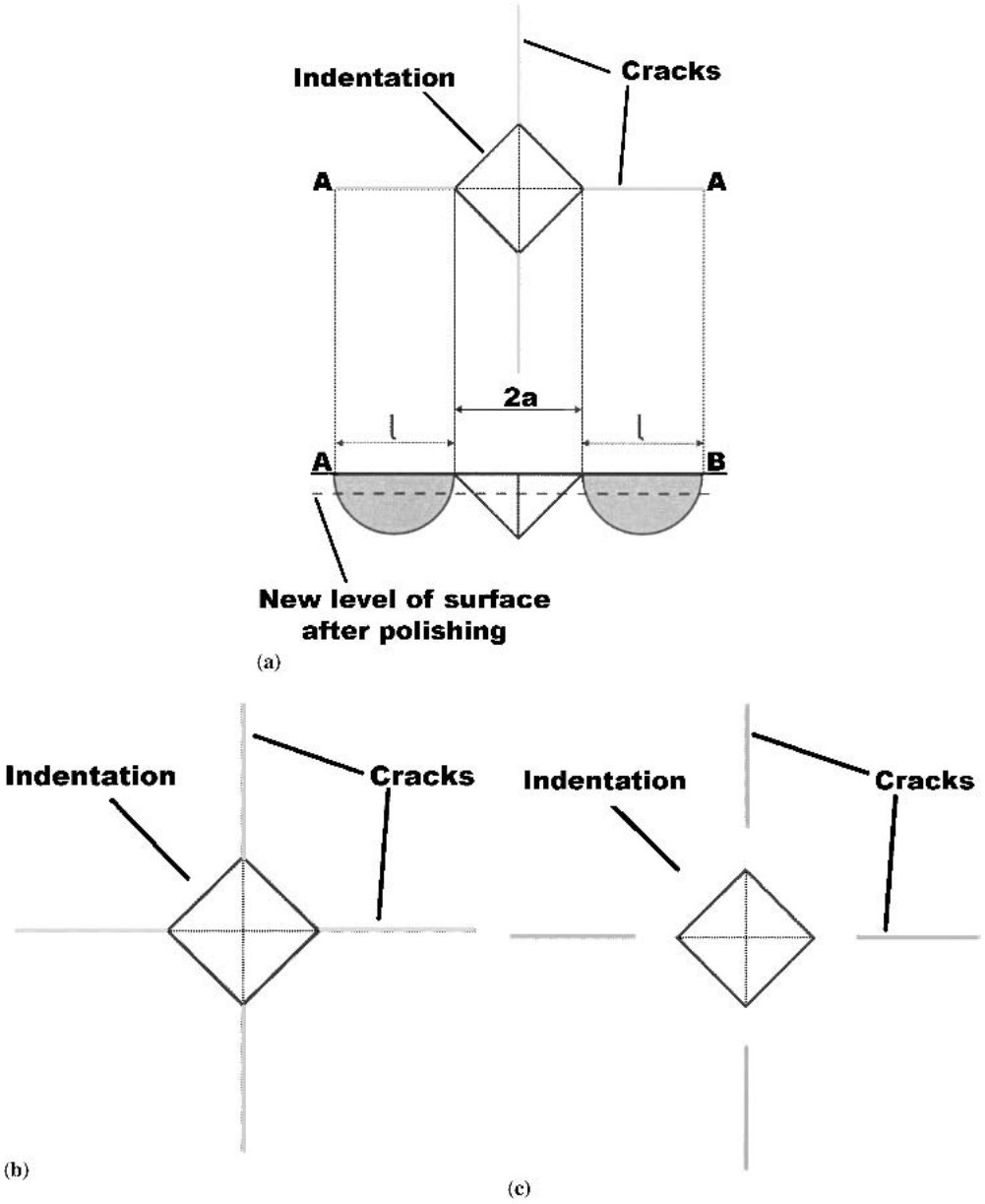

Fig. 4 **(a)** Schematic illustration of the Palmqvist crack system and supervision of the Palmqvist crack system **(b)** before and **(c)** after the serial sectioning

a Young's modulus of the coating parallel to the surface somewhat smaller than 100 GPa. This is in good agreement with the literature. References 11 and 12 report that the elastic modulus of similar materials can be five times smaller than the value of the material without defects.

The linear thermal expansion coefficient for molybdenum is $5.2 \times 10^{-6}\ K^{-1}$, which is smaller than that of the substrate material ($\sim 12 \times 10^{-6}\ K^{-1}$). This means that the positive quenching stresses[12] in the coating will be reduced by negative compression stresses induced by cooling from the fabrication temperature to room temperature. With x-ray measurements radial residual stresses of approximately 40 MPa were measured within the coating, whereas normal stresses were negligible. The measured values are comparable to values found in Ref. 8 and 13.

3. Experimental Methods

3.1 Determination of Local Material Properties

The examined composite is in first approximation a bimaterial consisting of the coating and the substrate material. In this case the local conditions in front of a crack are different from that in a homogeneous material. Furthermore the coating itself has a very inhomogeneous structure. To describe the fracture mechanical behavior of a material it is necessary to measure its local toughness properties, which requires special methods. Indentation toughness measurements are a useful tool for this purpose. The appearance of the cracks, which grow near to an indentation in a brittle material, is used to calculate the fracture toughness of the material.[14,15]

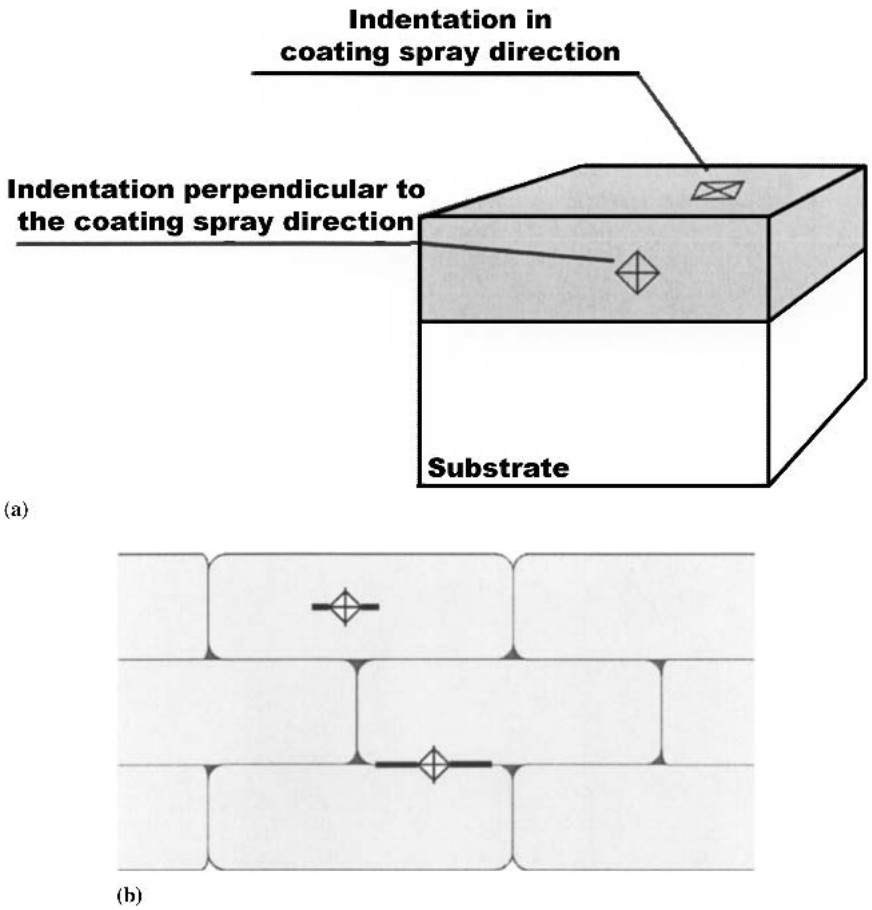

Fig. 5 Schematic illustration of **(a)** the definition of the indentation direction and **(b)** indentations into and between splats

Different types of crack systems may develop near the indentation. To identify the type, we used a method called serial sectioning.[16] For the examined material only the so-called Palmqvist type crack system was found, even for higher indentation loads were other crack systems can usually be observed.[17,18]

With Eq 2[19] it is possible to calculate a critical fracture toughness for Palmqvist cracks

$$K_c = k \cdot \frac{P}{a \cdot l^{1/2}} \qquad \text{(Eq 2)}$$

where k is a prefactor, which depends on the geometry of the used indenter and the examined material. The method used for the calculation of this parameter is described in Ref. 19. We performed indentation tests in the spray direction of the coating process (Fig. 5a) and perpendicular to that direction. Perpendicular to the spray direction it was possible to make indentations directly into the splats as well as between the splats revealing the difference between the toughness of the splats and the toughness of the interface between the splats.

For the Vickers indenter used and for the examined molybdenum we calculated values for the prefactor of $k = 0.011$ for indentations in the spray direction and $k = 0.015$ for indentations perpendicular to the spray direction.[19] For indentations perpendicular to the spray direction only two instead of four cracks were observed. This is the reason two different prefactors were necessary for these two indentation directions.

3.2 Determination of the Global Fracture Toughness

To study the global fracture toughness, special test samples were machined as can be seen in Fig. 6. The dimensions of the samples for the toughness test parallel to the coating-steel interface are width $W = 22.5$ mm, thickness $B = 9$ mm, height $2h = 15$ mm, depth of the starter crack $a = 7$ mm. The dimensions of the bending test samples are: height $H = 3$ to 5 mm, thickness $B = 3$ mm, span width $L = 23$ mm.

For examination of cracks parallel to the interface two coated steel beams were glued together using a multipurpose adhesive. In one of these two coatings, we produced a starter crack by spark erosion. The samples were loaded in the direction marked by two arrows in Fig. 6(a). In a standard tension test machine we determined the fracture toughness. During the test the load was measured and from the maximum load a standard fracture toughness value[20] was calculated. In-situ SEM experiments were done to study the path of the crack propagation.

Cracks perpendicular to the coating-steel interface were in-

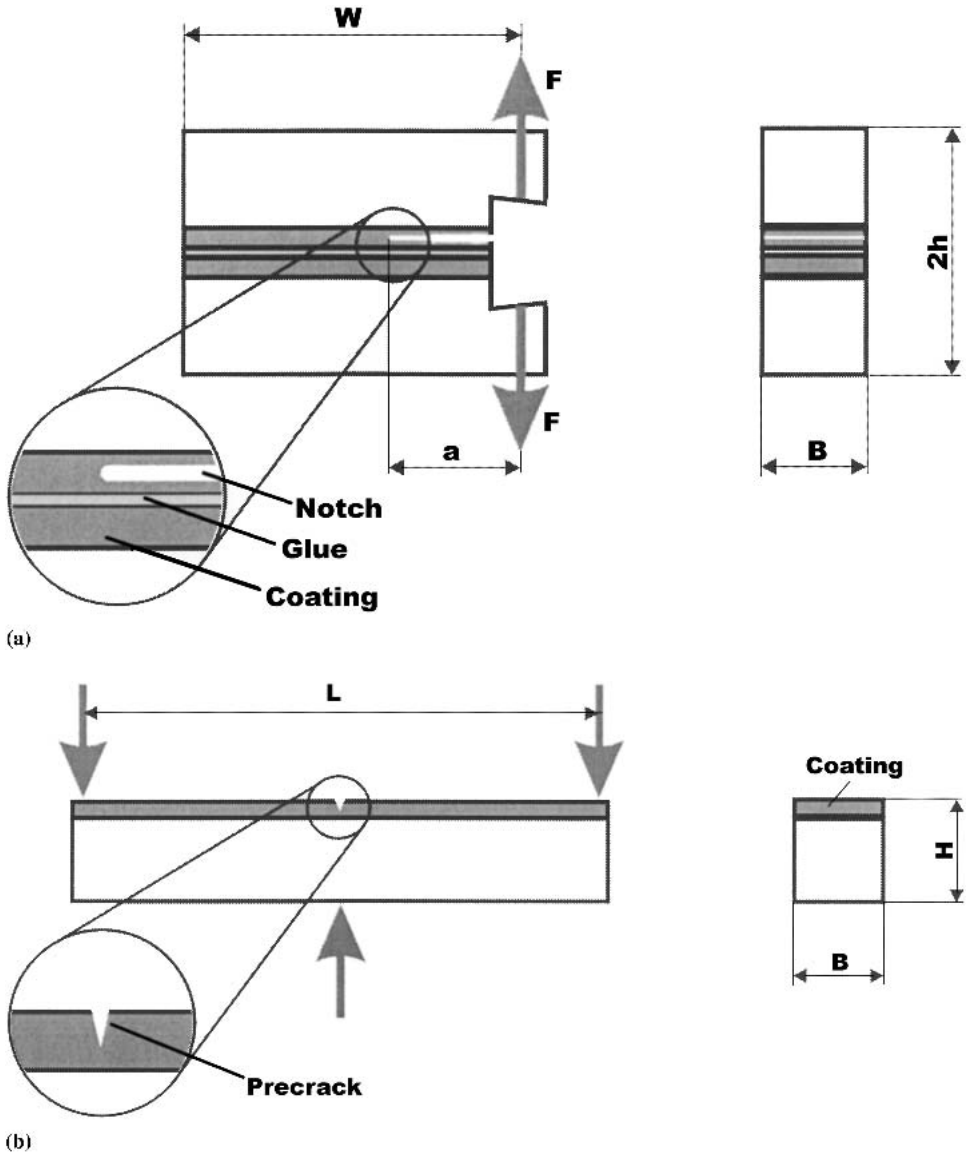

Fig. 6 Schematic illustration of the test samples for measuring the global fracture toughness: **(a)** specimens for cracks parallel to the interface, **(b)** notched bending test sample for cracks perpendicular to the interface

vestigated by three-point bending tests. A notch in the coating was produced by a special razor blade polishing technique.[21] The tests were performed in situ in the SEM to study the path of the crack propagation. The load at which the first crack propagation was detected was used to calculate a global fracture toughness value.

4. Results and Discussion

4.1 Some General Remarks on Cracks in Bimaterials

The local stress intensity in front of a crack in a bimaterial is usually different from the global stress intensity calculated by considering only the geometries of the specimen and the crack length and the applied load. The differences in the material properties can lead to elastic, plastic, and thermal mismatch.

A difference in Young's modulus and Poisson ratio in a bimaterial or a composite is called elastic mismatch. If in a bimaterial a crack propagates from the elastically weaker to the elastically stronger material the local stress intensity is smaller than the global stress intensity (i.e., the stress intensity in a homogeneous material) and vice versa.[5,22-25] A difference in the yield stress and/or the strain hardening exponent induces a plastic mismatch leading to reduction or increase of the local crack driving force only if the plastic zone reaches the interface of the two materials. If the crack approaches the interface from the plastically weaker to the plastically stronger material the local crack driving force is smaller than the global one and vice versa.[26-29] The difference in the thermal expansion coefficients is responsible for the thermal mismatch, which induces also a

difference between local and global crack driving force.[30,31] In general a reduction of the local crack driving force is called shielding and an increase is called antishielding.

4.2 Indentation Fracture Toughness

A few examples of cracks before and after the serial sectioning can be seen in Fig. 7. After the serial sectioning it is evident that the cracks are no longer connected to the edge of the indentation indicating that the crack system is of the Palmqvist type.

The results of the indentation fracture toughness tests are summarized in Table 1. For indentations perpendicular to the spray direction only two cracks can be determined (see Fig. 9). This can be explained by the layer-like structure of the molybdenum splats for indentations directly into the splats and by the layer-like structure of the coating itself for indentations in the interface between two splats. For indentations into a splat, this behavior is schematically shown in Fig. 8.

It is often reported that results of indentation fracture toughness tests are strongly influenced by the surface preparation method before the indentation. Therefore two kinds of surface preparation were applied. Both extensive mechanical polishing and electrolytic polishing led to identical results in the indentation toughness tests. In general the measured values tend to increase for small indentation loads due to an indentation size effect or R-curve effect of the toughness. For indentations perpendicular to the spray direction we measured higher values for indentations directly into the splats than for indentations between to splats. This indicates that the interface between the molybdenum splats is the weakest link in the coating. For indentations between the splats the values increase with the increasing indentation load, which may be induced by crack branching, which occurs more frequently at larger crack extensions.

In these tests the cracks propagate within the coating only, relatively far away from the coating substrate interface. The size of the plastic zone in front of the crack cannot be much larger then 1 μm for the observed critical stress intensity factor in

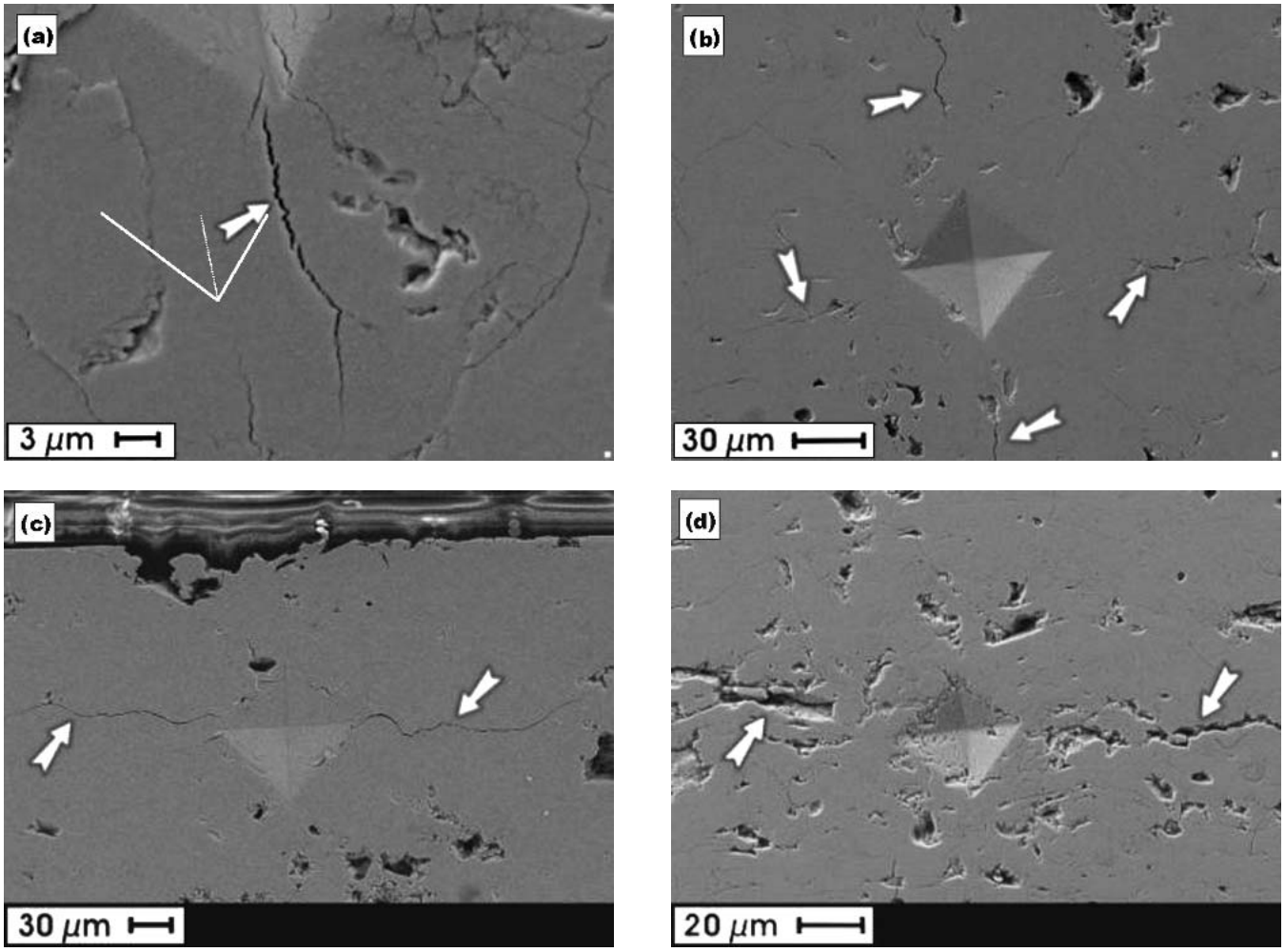

Fig. 7 Micrographs of indentation cracks; arrows mark the cracks. **(a)** One of four Palmqvist cracks of an indentation in spray direction; white lines trace the indentation edge. **(b)** Indentation cracks at an indentation in spray direction after serial sectioning; the cracks are no longer connected to the edge of the indentation. **(c)** Cracks of an indentation perpendicular to the spray direction; only two cracks can be recognized. **(d)** After serial sectioning it can be easily seen also that the cracks of indentations perpendicular to the spray direction are no longer connected to the edge of the indentation.[32]

the molybdenum coating; thus the plastic mismatch can be ignored.

The elastic mismatch cannot be ignored, however, if the crack length is much larger than the distance from the crack to the interface. If the crack length is comparable to its distance from the interface the amount of crack shielding is a few percent. The distance of the crack from the coating substrate interface was in the order of or smaller than the crack length. Hence the effect of the elastic mismatch[5] is smaller than the accuracy of the measured toughness values and therefore can be neglected.

In our case the residual stresses in the coating were of the tension kind. These stresses can lead to "shielding" if they act perpendicular to the crack propagation direction. This was not the case in the examined coatings where the residual stresses act parallel to the coating-substrate interface and therefore have no influence on the indentation cracks.

The Griffith toughness for molybdenum can be calculated to 1.1 MPa√m (E = 325 GPa and $2\gamma_e$ = 3.8 J/m^2[33]). A comparison of this value with the indentation toughness results shows that the coatings break almost ideally brittle.[1] The difference between measurement results of indentations in and perpendicular to the spray direction may stem from the microstructure of the splats or from the limited accuracy in the determination of the prefactors for the calculation of the toughness values from the indentation toughness tests.

[1]The fracture toughness of coarse grained Mo at room temperature is much larger (about 10 MPa√m). The grain size in the coating is very small, which may leat to low toughness values.

Table 1 Summary of the Indentation Toughness Test Results. Each Result is the Mean Value of at Least 5 Measurements. In All Cases the Standard Deviation Was Smaller Than 0.15 MPa√m for Indentations in the Spray Direction and Smaller Than 0.05 MPa√m for Indentations Perpendicular to the Spray Direction

Indentation Load, N	Place of Indentation	Indentation Direction	K_{IC}, MPa√m
1.16	Splat	I	0.93
29.43	Splat	I	1.17
49.05	Splat	I	1.35
98.10	Splat	I	1.39
0.41	Splat	P	1.23
0.80	Splat	P	0.81
1.16	Splat	P	0.72
9.81	Splat	P	0.60
0.41	Interface	P	0.46
0.80	Interface	P	0.29
9.81	Interface	P	0.31
19.62	Interface	P	0.41
29.43	Interface	P	0.50
49.05	Interface	P	0.53

Indentation direction: I, indentation in coating spray direction; P, indentation perpendicular to the coating spray direction

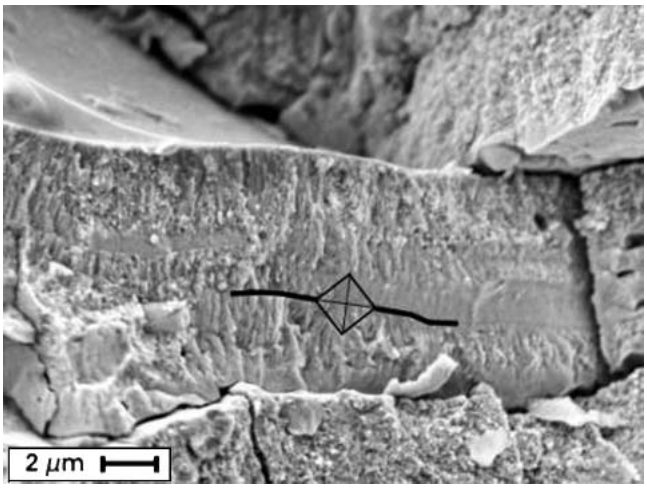

Fig. 8 Schematic sketch of the crack propagation direction for an indentation perpendicular to the spray direction drawn in a fractograph where the layered structure of the splats is visible. Only two cracks would be recognized after the indentation.

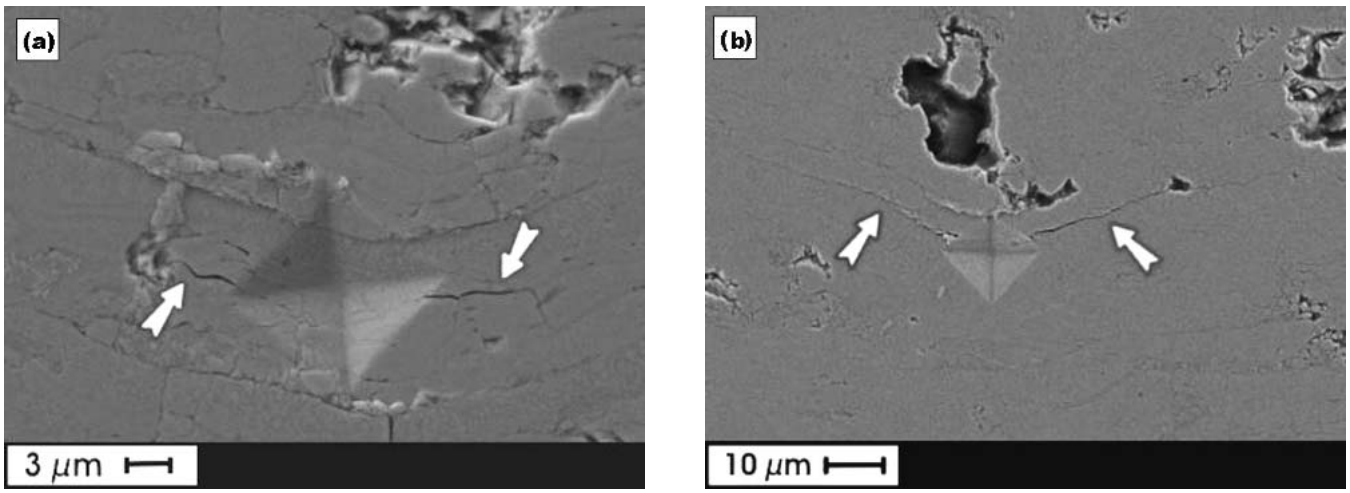

Fig. 9 Micrographs of indentations perpendicular to the spray direction with indentation loads smaller than 1 N: **(a)** indentation directly into a molybdenum splat, **(b)** indentation into the interface between two different splats.[32] Arrows mark the cracks.

4.3 Fracture Toughness Parallel to the Surface

Figure 10 illustrates the crack propagation during an in situ toughness experiment in a SEM. It is clearly evident that the crack propagates predominantly between the splats, as expected from the indentation experiments. Only in few cases the crack changes from one splat layer to another, which often occurs at preexisting thermal cracks in the splats. Such thermal cracks are clearly visible in Fig. 1, 2, and 11(a). Few of the splats, however, have to be fractured for this change of the crack path. The corresponding mechanism is schematically depicted in Fig. 12. The measured fracture toughness value for the crack parallel to the interface is 1.85 ± 0.2 MPa√m. This is significantly larger than the splat-splat toughness. What is the reason for this relatively large global toughness value? It is obvious that in addition to the splat-splat toughness the fracture of the splats contributes to the global toughness, however this cannot explain the large difference. One has to take into account that this is a composite. A shielding induced by the thermal and plastic mismatch does not occur or is negligible. The low value, however, of Young's modulus of the coating which is assumed to be 65 GPa, compared with that of the substrate steel of 210 GPa leads to a significant crack shielding induced by the elastic mismatch effect. Using a crack-shielding model of Hutchinson[35] (see appendix A) the amount of crack shielding can be calculated. With that model a ratio of Ktip/K = 0.542 can be obtained. K_{tip} is the local stress intensity in front of the crack, and K is the stress intensity in a comparably homogeneous material.

In a first approximation the global fracture toughness of the coating for a crack parallel to the interface can be calculated by

$$K_{IC} = (x \cdot K_{IC}^{G} + y \cdot K_{IC}^{S}) \cdot A \qquad \text{(Eq 3)}$$

where

K_{IC}^{G}	Splat-splat interface toughness (K_{IC} = 0.5 MPa√m)
K_{IC}^{S}	Toughness of a splat, Griffith toughness of the molybdenum (K_{IC} = 1.1 MPa√m)
x	Amount of the effect of splat-splat interface toughness on the global coating toughness
y	Amount of the effect of splat toughness on the global coating toughness, with $x + y = 1$
A	Crack shielding K/K_{tip} caused by the elastic mismatch, A = 1.85

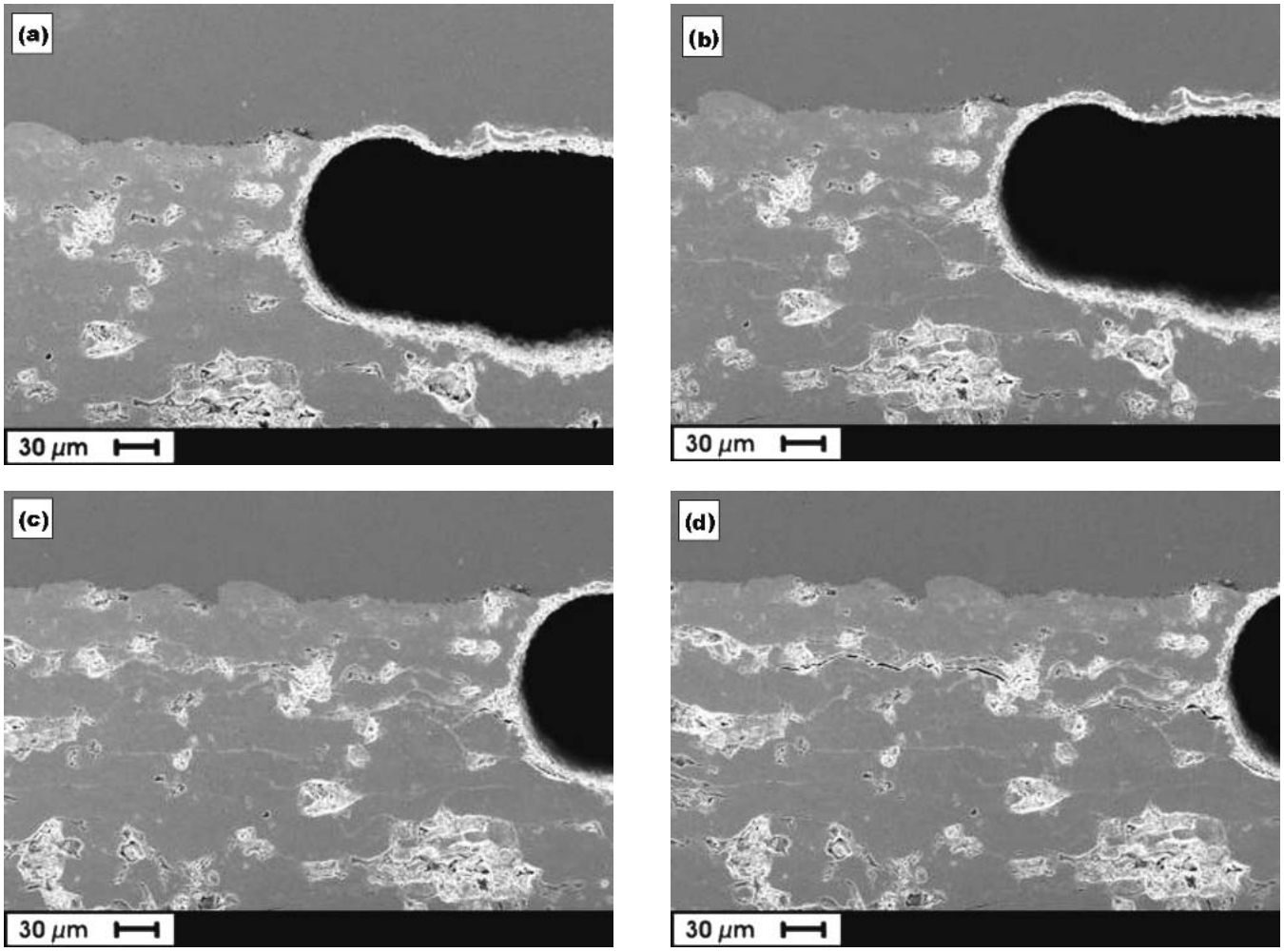

Fig. 10 Micrographs of an in situ toughness test: **(a)** root of the sparc-erosion starter notch without any loading; **(b-d)** with increasing load (300, 350, 400 N) a crack propagates from the root of the notch through the whole coating[32,34]

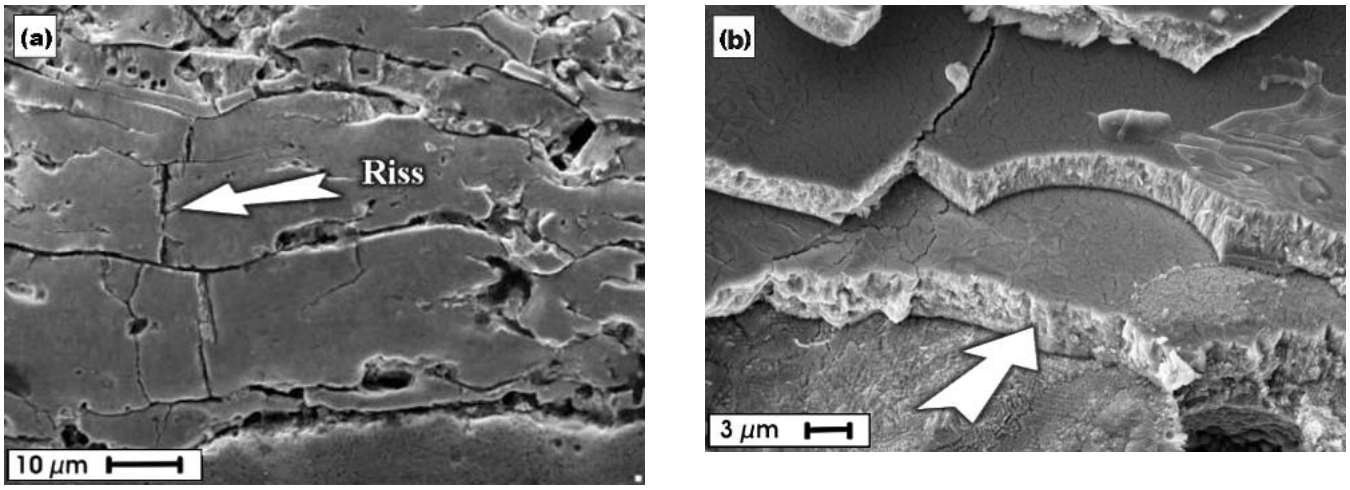

Fig. 11 Micrographs of the molybdenum coating: **(a)** electrolytic etched cross-section of the coating; the thermal cracks in the coating can easily be seen. **(b)** Crack surface of the coating after a fracture toughness test; the main part of the crack propagation takes place in the interface between two splats. An arrow marks the crack propagation direction.

Equation 3 gives the contribution to the toughness from the splat-splat interface and the fracture of splats and the contribution of the elastic shielding. If we assume x and y both to be 0.5, a global fracture toughness of 1.49 MPa√m can be calculated. The measured value is higher than the estimated one. Hence the contribution of the toughness of the splats to the global toughness must be more than the assumed 50%. An additional contribution to the crack shielding may stem from crack branching, which is not taken into account by this simple model.

4.4 Cracks Perpendicular to the Surface

Figure 13 illustrates the crack propagation during an in situ three-point bending experiment in a SEM. The failure of the weak interface between the splats leads to the building of a crack network in front of the notch (pre-crack) of the test samples. Therefore the model from Sigl[36] (Appendix B) can be used to estimate the global fracture toughness, which should be measured in the bending tests.

For these tests only the elastic and the thermal mismatch are of interest. The plastic mismatch can be neglected due to the small size of the plastic zone in molybdenum in front of a crack. Using the stress intensity handbook,[5] a ratio of $K_{tip}/K = 0.67$ for the observed crack-interface arrangement can be estimated. The following parameters are used to calculate a ΔK_t of 0.5 MPa√m.

K_0 = 1.1 MPa√m	Griffith-toughness of the coating
f = 25%	Defect ratio of 25%. Due to microcracking this value should be higher than the measured coating porosity of approximately 10%
$\beta^* = 1.15$, $\gamma^* = 1.4$	For ν of 0.2 (Fig. 15)
σ_R = 40 MPa	Residual stresses in the coating
h = 100 µm	Size of the microcrack zone in front of the pre-crack

Equation 4 can be used to estimate the global fracture toughness of the coating for cracks perpendicular to the coating substrate interface:

$$K_{IC} = (K_0 + \Delta K_r) \cdot \frac{K_{tip}}{K} \quad \text{(Eq 4)}$$

K_0 is the intrinsic fracture toughness (Griffith-toughness) of the coating material. The calculated global fracture toughness is then 2.4 MPa√m. For the load at which the first crack propagation can be observed during the tests a fracture toughness of approximately 3 MPa√m was observed. Due to the microstructure and the defects in the coating the first crack propagation during the test is not easy to detect therefore the determined toughness value is only an approximation. Taking into account these uncertainties, the accordance between the estimated and the measured value is relatively good.

5. Conclusion

The fracture behavior of thick flame sprayed molybdenum coatings was investigated. Special fracture mechanics tests were made to study the global fracture behavior of cracks parallel and perpendicular to the coating substrate interface. By means of indentation fracture toughness tests the local behavior of the material was also examined.

The fracture toughness determined by indentation tests for a crack propagation direction perpendicular to the surface is about 1 MPa√m, which is approximately equal to the Griffith toughness of molybdenum. The local fracture toughness parallel to the surface is somewhat smaller, and the local fracture toughness of the splat-splat interface is significantly smaller than the Griffith toughness of Mo (about 0.5 MPa√m). Hence, the splatsplat interfaces are the weakest part in the microstructure. The global fracture toughness is about 2 MPa√m for crack propagation parallel to the substrate-coating interface and about 3 MPa√m perpendicular to that interface. The relatively large difference between the global toughness and the splat-splat toughness can be explained by a certain contribution of necessary fracture of the splats, the elastic mismatch (and thermal mismatch for cracks perpendicular to the interface), and some contributions

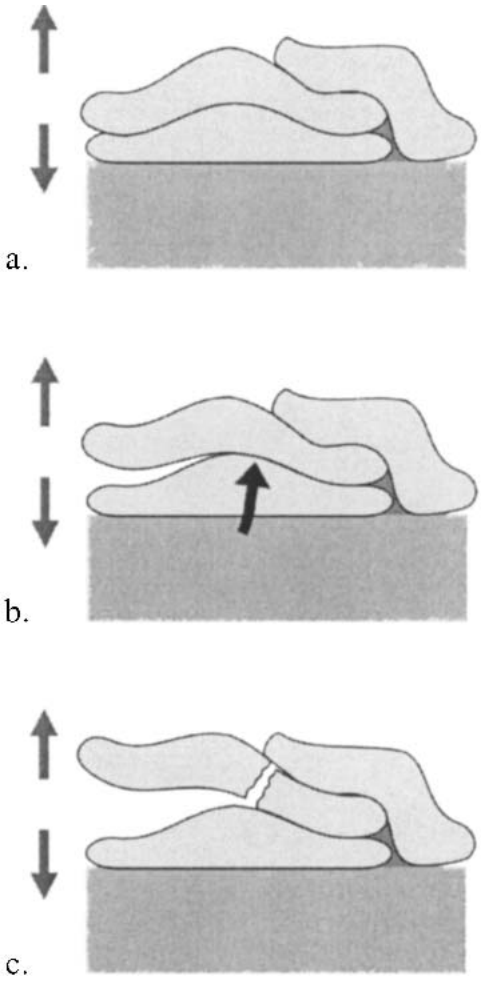

Fig. 12 Schematic sketch of the breaking of a splat: **(a)** under load a crack propagates in the interface between two splats. **(b)** The crack propagates to a certain length where a further propagation is hindered, for example by another overlapping splat. **(c)** If the bending moment rises high enough, this splat will break. Thermal cracks will force this effect. The sketch is reduced to a two-dimensional problem whereas in the real coating it is a complex three-dimensional problem.

which come from the geometry (crack deflection and crack branching).

Acknowledgments

This work was funded by the European Community under the Industrial and Materials technologies programme (BRITE/EURAM III). The authors are thankful to the coating company Flametal S.p.a. now Praxair Surface Technologies for providing us with the coated specimens and also to all other project partners for their assistance.

Appendix A

Elastic Mismatch for Cracks Perpendicular to the Coating-Substrate Interface

Hutchinson[35] developed a model for the case shown in Fig. 14 to estimate the crack tip shielding. The model was derived for

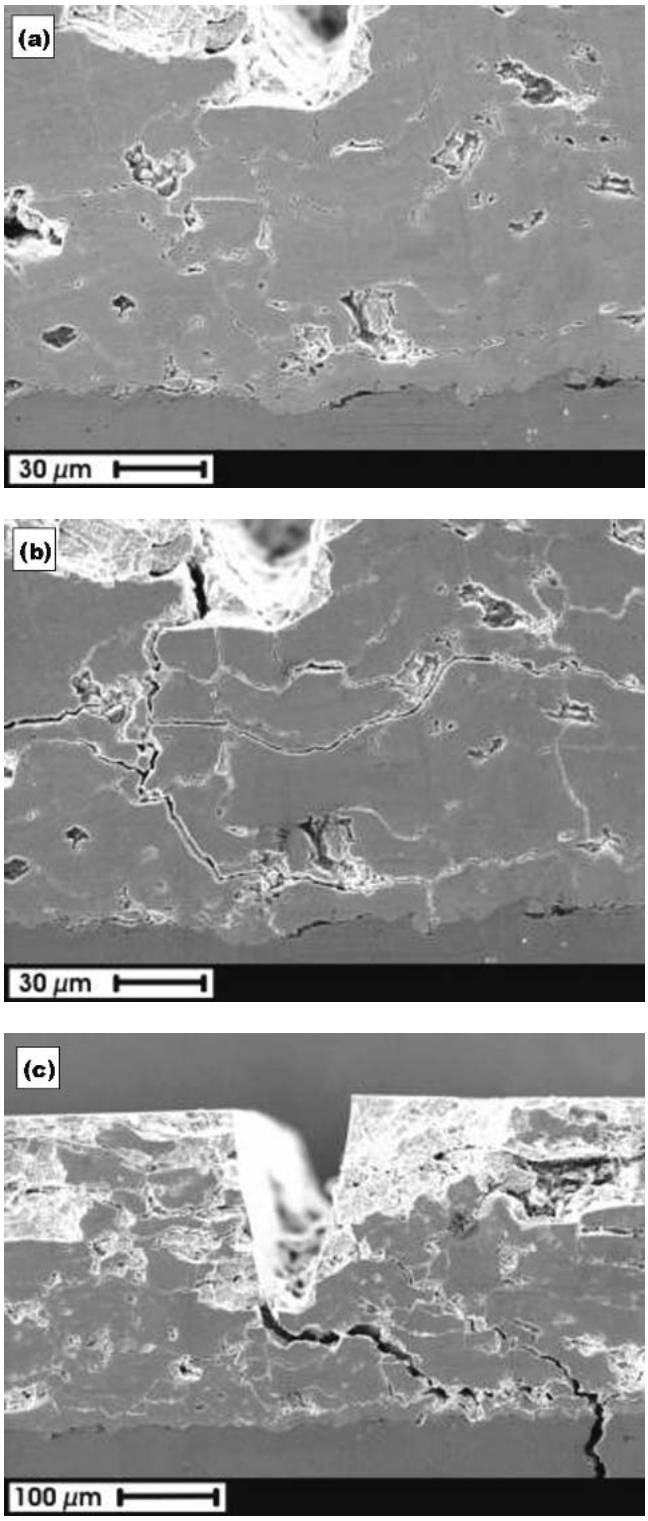

Fig. 13 SEM of the notch tip region taken during an in situ bending test: **(a)** pre-crack in the Mo-coating, **(b)** crack network in the coating[86] at a load of 2.0 kN, **(c)** failure of the substrate material at a load of 2.15 kN

a material with a microcrack process zone near a crack. The shielding is forced by the change of the Young's modulus due to the building of micro cracks. That is very similar to the investi-

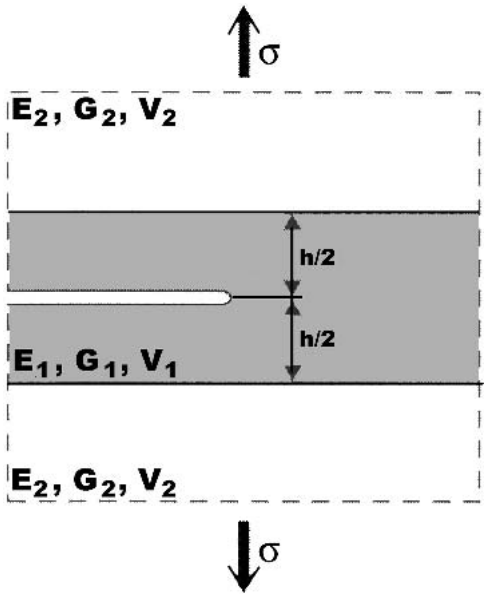

Fig. 14 Schematic of a crack with a completely developed microcrack process zone, a zone with a reduced elastic modulus[35]

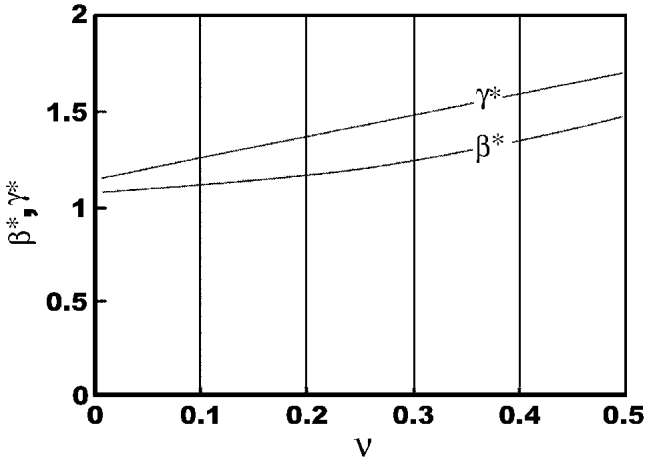

Fig. 15 Dependence of the parameters β* and γ* on Poisson's ratio ν for a completely developed microcrack process zone[36]

gated coating substrate problem, where the Young's modulus in the coating is reduced by defects.

The following formulas are used to estimate the crack tip shielding.

Hutchinson defines two moduli parameters

$$\delta_1 = \frac{1}{1-\nu_2} \cdot \left[\frac{G_2}{G_1} - 1\right] \tag{A1}$$

$$\delta_2 = \frac{1}{1-\nu_2} \cdot \left[\nu_1 \cdot \frac{G_2}{G_1} - \nu_2\right] \tag{A2}$$

The shear modulus G_2 and the Poisson ratio ν_2 are properties of the substrate material. G_1 and ν_1 are the comparable properties of the material with micro cracks. For the estimation of the crack shielding for the case shown in Fig. 14 Hutchinson gives the following equation

$$\frac{K_{tip}}{K} = [1 + \delta_1 - \delta_2]^{-1/2} \tag{A3}$$

for an elastically isotropic material with a completely developed microcrack zone.

Appendix B

Crack Tip Shielding Forced by Microcracks

Generated microcracks can induce crack tip shielding and so reduce the residual stresses in front of the crack. A model which considers this effect was suggested by Sigl.[36] The local stress intensity in front of a crack can be described as follows:

$$K_{tip} = K - \Delta K_t \tag{B1}$$

K is the global stress intensity and ΔK_t is the amount of the crack tip shielding. In the model of Sigl ΔK_t is divided into two parts:

$$\Delta K_t = \Delta K_d + \Delta K_m \tag{B2}$$

K_d is the part, which is induced by the reduction of the residual stresses in front of the main crack, caused by the production of micro cracks and ΔK_m stems from the change in the Young's modulus in front of the main crack. These parts can be calculated as follows:

$$\Delta K_d = f \cdot \gamma^* \cdot \sigma_R \cdot \sqrt{h} \tag{B3}$$

$$\Delta K_m = f \cdot \beta^* \cdot K_0 \tag{B4}$$

where *f is* the defect volume in percent, which is given by $f = N \cdot b^3$.[35] N is the number of cracks in a unit cell and b is the radius of the cracks. γ* and β* are parameters, which depend on Poisson's ratio ν of the material and can be taken from Fig. 15. σ_R denotes the residual stresses and h describes the size of the micro crack process zone. These equations can be used to calculate the crack tip shielding in a material, which tends to build micro cracks in front of a crack.

References

1. R.B. Heimann: *Plasma-Spray Coating,* Wiley/VCH, Weinheim, Germany, 1996.
2. J.M. Tura, A. Traveria, M.D. Castellar, J. Pujada, J. Blouet, R. Gras, H.G. Magham, P. Belair, T. Hanau, A. Romero: "Frictional Properties and Wear of a Molybdenum Coating and a Bronze (Cu-10%Sn) With Friction Modifier Fillers," *Wear*, 1995, *189,* pp. 70-76.
3. S. Sampath, S. Usmani, and D.L. Houck: "Applications of Mo and Mo-Alloys as Thermal Spray Coatings, Molybdenum and Molybdenum Alloys," *TMS Annual Meeting,* A. Crowson, E.S. Chen, J.A. Shields and P.R. Subramanian, ed., TMS, Warrendale, 1998, pp. 145-54.
4. P.J. Callus and C.C. Berndt: "Relationship Between the Mode II Fracture Toughness and Microstructure of Thermal Spray Coatings," *Surf. Coat. Technol.*, 1999, *114,* pp. 114-28.
5. Anon: *Stress Intensity Factors Handbook,* Y. Murakami, ed., Pergamon Press, Oxford, 1992.

6. S. Scherer, M. Gruber, J. Stampfl, and O. Kolednik: "Automatische 3D-Oberflächenrekonstruktion aus Stereoskopischen Rasterelektronenmikroskop-Aufnahmen," 1. Tagung des DVM-Arbeitskreises Mikrosystemtechnik, Micro Maf 95, Berlin, Germany, B. Michel and T. Winkler, ed., 1995, pp. 671-76 (in German).
7. J. Stampfl, Ch.O.A. Semprimoschnig, and O. Kolednik: "Topometrie Metallischer Bruchoberflächen," 17. Tagung des DVM-Arbeitskreises Rastermikroskopie in der Materialprüfung, Berlin, Germany, H. Vetters, ed., Halle/Saale, 1996, pp. 179-84 (in German).
8. J. Matejicek and S. Sampath: "Intrinsic Residual Stresses in Single Splats Produced by Thermal Spray Process," *Acta Mater.*, 2001, *49,* pp. 1993-99.
9. I. Sevostianov and M. Kachanov: "Modelling of Anisotropic Elastic Properties of Plasma-Sprayed Coatings in Relation to Their Microstructure," *Acta Mater.*, 2000, *48,* pp. 1361-70.
10. S.H. Leigh and C.C. Berndt: "Modelling of Elastic Constants of Plasma Spray Deposits With Ellipsoid-Shaped Voids," *Acta Mater*., 1999, *47,* pp. 1575-86.
11. R.J. Damani and A. Wanner, "Microstructure and Elastic Properties of Plasma-Sprayed Alumina," *J. Mater. Sci.*, 2000, *35,* pp. 4307-18.
12. O. Kesler, J. Matejicek, S. Sampath, S. Suresh, T. Gnaeupel-Herold, P.C. Brand, and H.J. Prask: "Measurement of Residual Stress in Plasma-Sprayed Metallic, Ceramic and Composite Coatings," *Mater. Sci. Eng.*, 1998, *A257,* pp. 215-24.
13. X. Jiang, S. Sampath, and H. Herman: "Grain Morphology of Molybdenum Splats Plasma-Sprayed on Glass Substrates," *Mater. Sci. Eng.*, 2001, *A299,* pp. 235-40.
14. C.B. Ponton and R.D. Rawlings: "Vickers Indentation Fracture Toughness Test, Part 1. Review of Literature and Formulation of Standardized Indentation Toughness Equations," *Mater. Sci. Technol.*, 1989, *5,* pp. 865-72.
15. C.B. Ponton and R.D. Rawlings: "Vickers Indentation Fracture Toughness Test, Part 2. Application and Critical Evaluation of Standardized Indentation Toughness Equations," *Mater. Sci. Technol.*, 1989, *5,* pp. 961-76.
16. T. Lube: "Indentation Crack Profiles in Silicon Nitride," *J. Eur. Ceram. Soc.*, 2001, *21,* pp. 211-18.
17. K.K. Sharma, P.N. Kotru, R.N. Tandon, and B.M. Wanklyn: "Hardness and Dielectric Characteristics of Flux Grow Terbium Aluminate Crystals," *Mater. Sci. Eng.*, 1999, *B57,* pp. 197-208.
18. K. Nihara, R. Morena, and D.P.H. Hasselman: "Evaluation of K_{IC} of Brittle Solids by the Indentation Method With Low Crack-to-Indent Ratios," *J. Mater. Sci. Lett.,* 1982, *1,* pp. 13-16.
19. D.K. Shetty, I.G. Wright, P.N. Mincer, and A.H. Clauer: "Indentation Fracture of WC-Co Cermets," *J. Mater. Sci.*, 1985, *20,* pp. 1873-82.
20. ASTM Standard E399-90: Standard Test Method for Plain-Strain Fracture Toughness of Metallic Materials, American Society for Testing and Materials, Philadelphia, PA, 1993.
21. R.J. Damani, Ch. Schuster, and R. Danzer: "Polished Notch Modification of SENB-S Fracture Toughness Testing," *J. Eur. Ceram. Soc.*, 1997, *17,* pp. 1685-89.
22. T.S. Cook and F. Erdogan: "Stresses in Bonded Material With a Crack Perpendicular to the Interface," *Int. J. Eng. Sci.*, 1972, *10,* pp. 677-97.
23. F. Erdogan and V. Biricikoglu: "Two Bonded Half Planes With a Crack Going Through the Interface," *Int. J. Engng. Sci.*, 1973, *11,* pp. 745-66.
24. R.O. Ritchie, R.M. Cannon, B.J. Dalgleish, R.H. Dauskardt, and J.M. McNaney: "Mechanics and Mechanisms of Crack Growth at or Near Ceramic-Metal Interfaces: Interface Engineering Strategies for Promoting Toughness," *Mater. Sci. Eng.*, 1993, *A166,* pp. 221-35.
25. A.G. Evans, M. Rühle, B.J. Dalgleish, and P.G. Charalambides: "The Fracture Energy of Bimaterial Interfaces," *Mater. Sci. Eng.*, 1990, *A126,* pp. 53-64.
26. Y. Sugimura, P.G. Lim, C.F. Shih, and S. Suresh: "Fracture Normal to a Bimaterial Interface: Effect of Plasticity on Crack-Tipp. Shielding and Amplification," *Acta Mater.*, 1995, *43*(3), pp. 1157-69.
27. R. Pippan and F.O. Riemelmoser: "Fatigue of Bimaterials: Investigation of the Plastic Mismatch in Case of Cracks Perpendicular to the Interface," *Comp. Mat. Sci.*, 1998, *13,* pp. 108-16.
28. R. Pippan, K. Flechsig, and F.O. Riemelmoser: "Fatigue Crack Propagation Behavior in the Vicinity of an Interface Between Materials With Different Yield Stresses," *Mater. Sci. Eng.*, 2000, A283, pp. 225-33.
29. R. Pippan, K. Flechsig, F.O. Riemelmoser, and H.P. Brantner: "Fatigue Crack Propagation Perpendicular to an Interface: The Effect of Plastic Mismatch," *13th European Conference on Fracture,* M. Fuentes, M. Elices, A. Martin-Meizos, and J.&M. Martinez-Esnaola, Elsevier, Surrey, UK, 2000, 85cl.pdf (CD).
30. I. Iordanova and K.S. Forcey: "Texture and Residual Stresses in Thermally Sprayed Coatings," *Surf. Coat. Technol.*, 1997, *91,* pp. 174-82.
31. J. Matejicek, S. Sampath, P.C. Brand, and H.J. Prask: "Quenching, Thermal and Residual Stress in Plasma Sprayed Deposits," *Acta Mater.*, 1999, 47(2), pp. 607-17.
32. H.P. Brantner, R. Pippan, W. Prantl, S. Bertini, and O. Lacroix: "Bruchverhalten Flammgespritzter Molybdänschichten," 33. Tagung DVM-Arbeitskreis Bruchvorgänge, H.A. Richard, ed., Paderborn, Germany, 2001, pp. 133-42 (in German).
33. K-H. Schwalbe, *Bruchmechanik metallischer Werkstoffe,* Hanser, München Wien, 1980 (in German).
34. H.P. Brantner, R. Pippan, W. Prantl, S. Bertini, and O. Lacroix: "Fracture Mechanical Behavior of PLASMA-Sprayed Coatings," *13th European Conference on Fracture,* M. Fuentes, M. Elices, A. Martin-Meizos, and J.&M. Martinez-Esnaola, ed., Elsevier, Surrey, UK, 2000, 61cl.pdf (CD).
35. J.W. Hutchinson: "Crack Tip: Shielding by Micro-Cracking in Brittle Solids," *Acta Mater.*, 1987, *35*(7), pp. 1605-19.
36. L.S. Sigl: "Microcrack Toughening in Brittle Materials Containing Weak and Strong Interfaces," *Acta Mater.*, 1996, *44*(9), pp. 3599-609.